



Conti, S., Vila, B., Sellés, A. G., Galobart, À., Benton, M. J., & Prieto-Márquez, A. (2020). The oldest lambeosaurine dinosaur from Europe: Insights into the arrival of Tsintaosaurini. *Cretaceous Research*, 107, [104286]. <https://doi.org/10.1016/j.cretres.2019.104286>

Peer reviewed version

License (if available):  
CC BY-NC-ND

Link to published version (if available):  
[10.1016/j.cretres.2019.104286](https://doi.org/10.1016/j.cretres.2019.104286)

[Link to publication record in Explore Bristol Research](#)  
PDF-document

This is the author accepted manuscript (AAM). The final published version (version of record) is available online via Elsevier at <https://www.sciencedirect.com/science/article/pii/S0195667119301879#:~:text=Hollow%2Dcrested%20lambeosaurine%20hadrosaurids%20represent,distribution%20during%20the%20Late%20Cretaceous> . Please refer to any applicable terms of use of the publisher.

## University of Bristol - Explore Bristol Research

### General rights

This document is made available in accordance with publisher policies. Please cite only the published version using the reference above. Full terms of use are available: <http://www.bristol.ac.uk/red/research-policy/pure/user-guides/ebr-terms/>

**The oldest lambeosaurine dinosaur from Europe: insights into the arrival of  
Tsintaosaurini**

**Simone Conti<sup>a</sup>, Bernat Vila<sup>b,c,d</sup>, Albert G. Sellés<sup>b,c</sup>, Àngel Galobart<sup>b,c</sup>, Michael J. Benton<sup>a</sup>,  
Albert Prieto-Márquez<sup>a,b\*</sup>,**

<sup>a</sup> School of Earth Sciences, University of Bristol, Life Sciences Building, 24 Tyndall Avenue,  
Bristol BS8 1TQ, United Kingdom

<sup>b</sup> Institut Català de Paleontologia Miquel Crusafont, Universitat Autònoma de Barcelona,  
Carrer de l'Escola Industrial 23, 08201 Sabadell, Barcelona, Spain

<sup>c</sup> Museu de la Conca Dellà-Parc Cretaci, Carrer del Museum 4, 25650 Isona, Lleida, Spain

<sup>d</sup> Departament de Geologia, Facultat de Ciències, Universitat Autònoma de Barcelona, Carrer  
de l'Eix central, 08193, Cerdanyola del Vallès, Barcelona, Spain

*\*Corresponding author. E-mail: [redshore@gmail.com](mailto:redshore@gmail.com)*

## Abstract

The hollow-crested lambeosaurine hadrosaurids represent one of the latest and most rapid radiations of ornithischian dinosaurs, attaining a nearly global distribution during the Late Cretaceous. Although their presence in Europe is well documented, there are questions about the origin and timing of their arrival in this continent. The analysis of old and newfound lambeosaurine specimens from the Els Nerets locality (eastern Tremp Syncline, northeastern Spain) have shown that the ornithopod dinosaurs from this classic site belong to Lambeosaurinae. Recent chronostratigraphic data places the locality in the lower Maastrichtian, implying that the Els Nerets lambeosaurine is the first occurrence of the clade in Europe. The Els Nerets lambeosaurine exhibits some noticeable pelvic features only shared with the Asian taxon *Tsintaosaurus spinorhinus* and thus we hypothesize a close taxonomic affinity between the lambeosaurine from Els Nerets and the Eurasian Tsintaosaurini. Members of this tribe would have dispersed into the Ibero-Armorican Domain not later than the early Maastrichtian, coexisting with endemic dinosaurian groups for some time.

**Keywords:** anatomy, phylogeny, biogeography, Cretaceous, Hadrosauridae, Lambeosaurinae

## 1. Introduction

European Late Cretaceous dinosaurs have been described from Austria, Belgium, Germany, Hungary, Italy, Portugal, Slovenia, Sweden, the Netherlands (Buffetaut, 2009; Dalla Vecchia, 2014; Csiki-Sava et al., 2015), and more prominently from the Hațeg Basin of Romania (Benton et al., 2010; Csiki-Sava et al., 2015), Spain (Puértolas-Pascual et al., 2018; Canudo et al., 2016; Cruzado-Caballero et al., 2010, 2013; Company et al., 2015; Pereda-Suberbiola et al., 2009), and southern France (Csiki-Sava et al., 2015; Dalla Vecchia, 2014; Dalla Vecchia et al., 2014; Prieto-Márquez et al., 2013). Among the various clades recorded in this region of the Globe, lambeosaurine hadrosauroids are probably the most commonly found (Pereda-Suberbiola et al., 2009; Cruzado-Caballero et al., 2010; Prieto-Márquez et al., 2013; 2019; Dalla Vecchia et al., 2014; Fondevilla et al., 2018). Specifically, they are uniquely found in the Ibero-Armorican domain, the largest island of the Late Cretaceous European archipelago. In this region their stratigraphic distribution is restricted to the Maastrichtian, while worldwide their fossils range from Santonian to the upper Maastrichtian strata in Asia and North America (Prieto-Márquez, 2010). European hadrosaurids are so far represented by five species, four of them from the late Maastrichtian: *Pararhabdodon izonensis* Casanovas-Cladellas et al., 1993; *Arenysaurus ardevoli* Pereda-Superbiola et al., 2009; *Blasisaurus canudo* Cruzado-Caballero et al., 2010, *Canardia garonnensis* Prieto-Márquez et al., 2013 and one from the early Maastrichtian *Adynomosaurus arcanus* Prieto-Márquez et al., 2019.

To date, the appearance of lambeosaurine dinosaurs in the Ibero-Armorican island, and therefore in the European archipelago is dated “sometime during the Maastrichtian” (Prieto-Márquez et al., 2013, p. 1). However, tsintaosaurin osteological data was lacking from lower Maastrichtian sites. The presence of hadrosaurids at that time had a significant impact on the reorganization of vertebrate faunas during the latest Cretaceous of southwestern Europe,

coinciding with the final stages of the faunal turnover interval (Vila et al., 2016; Fondevilla et al., 2019).

In the context of this temporal and palaeobiogeographic scenario, we revisited the lower Maastrichtian locality of Els Nerets, in the eastern Tremp syncline (NE Spain). We review the previously published material of hadrosaurids and describe new fossils of this clade in order to reassess a possible first occurrence of lambeosaurine fossils in Europe and their arrival from Asia. Further, recent chronostratigraphic calibrations in the region indicate that the site is important as the oldest in western Europe preserving unequivocal evidence of hadrosaurids, as part of a diverse and transitional ecosystem composed of plants and palynomorphs (Torices et al., 2012), fishes (Blanco et al., 2017), turtles, crocodylians (Buscalioni et al., 1986, Blanco, 2017), as well as theropod, ankylosaurian, and sauropod dinosaurs (Casanovas et al., 1987; Riera et al., 2009; Dalla Vecchia et al., 2014).

**Institutional abbreviations**—**AEMH**, Amur Natural History Museum, Blagoveschensk, Russia; **CMN**, Canadian Museum of Nature, Ottawa, Canada; **FMNH**, The Field Museum, Chicago, U.S.A; **IPS**, Institut Català de Paleontologia Miquel Crusafont, Sabadell, Spain; **IVPP**, Institute of Vertebrate Paleontology and Paleoanthropology, Beijing, China; **LACM**, Natural History Museum of Los Angeles County, Los Angeles, U.S.A; **MCD**, Museu de la Conca Dellà, Isona, Spain; **MDE**, Musée des Dinosauriens d'Espérance, France; **MOR**, Museum of the Rockies, Bozeman, U.S.A; **MPZ**, Museo Paleontológico de la Universidad de Zaragoza, Zaragoza, Spain.

## **2. Els Nerets locality**

### *2.1 Geological Setting*

The locality of Els Nerets is located 500 m north of Vilamitjana village, near the town of Tremp (Lleida province, northwestern Catalonia; Fig. 1). The locality exposes deposits of La Posa Formation of the Tremp Group (Fig. 2), in the Tremp syncline, one of the four Cretaceous basins that occur in the southern Pyrenees (Fig. 1). The Maastrichtian to Thanetian materials of the Tremp Group (Mey et al., 1968) are widely exposed in the southern flank of the Pyrenees, overlying or interfingering to the east with the Arén Sandstone Formation, recording a regressive trend that started at the Campanian-Maastrichtian boundary (Rosell et al., 2001). The Tremp Group has been divided into four units, from the base to the top as follows: 1) La Posa Formation (Cuevas, 1992), also referred to as “Grey Unit” or “Grey Garumnian” (Rosell et al., 2001), consisting of alternations of grey marlstones and sandstones, deposited in lagoon settings with mudflats, freshwater lakes and marshes; 2) Conques Formation (Cuevas, 1992), also referred to as “Lower Red Unit”, consisting of reddish and brownish mudstones deposited in floodplains and fluvial deposits with tidal influence; 3) Talarn Formation (Cuevas, 1992), also referred to as “Vallcebre limestones”, consisting of sandstones and conglomerates deposited in lacustrine environments, and 4) Suterranya Formation (Cuevas, 1992), also referred to as “Upper Red Unit”, an alternation of limestones and mudstones deposited in a fluvial-alluvial environment. Stratigraphic data (biostratigraphy, magnetostratigraphy and correlation with other units) indicate a Maastrichtian age for the Cretaceous portion of the Tremp Group (La Posa and Conques Formations) in the Tremp syncline (Diez-Canseco et al., 2014; Fondevilla et al., 2017; Riera et al., 2009, Villalba-Breva and Martin-Closas, 2013).

The site of Els Nerets is lateral to the Vicari section, noted by Torices et al. (2012). There the authors identified three stratigraphic units through the 42 m stratigraphic section: the Arén Sandstone Formation is present as the lowermost and the uppermost units, composed of clean, mature, mixed carbonate-cemented shoreface-to-near-shore arenite with rudists and

grey offshore marls with inoceramids; the top of this bed is composed of middle-grained hybrid arenite modified by reddish-ochre mottling and iron crusts containing abundant dinosaur eggshells and isolated bones; the uppermost unit is formed from marine calcarenites and sandy limestones showing wackestone-packestone texture and wavy cross stratification. The two Arén Sandstone Formation units are separated by La Posa Formation strata belonging to the Tresp Group, which changes notably from East to West, forming a local furrow or lens-shaped geometry with a maximum thickness around 40 m. The lower 21 m thick portion mostly consists of grey mudstones. In its middle part, the mudstone evolves into a grey sandstone showing a well-developed paleosol at the top. Approximately one metre above the paleosol, a one metre thick marly limestone occurs. The fossils herein were found at the base of this marly limestone bed. The upper 15 m thick portion of the Tresp Group is composed of ochre and purple mudstones. Based on lithological and palynological content, three transgressive-regressive episodes have been identified (Torices et al., 2012), with the Arén Sandstone Formation representing fully marine deposition, whereas the Tresp Group beds suggest a lagoonal environment that evolved to more drained conditions in its upper portion. The dominance of planktonic marine organisms near the top of the grey unit indicates a dramatic transgression that was not recorded in the lithology (Torices et al., 2012). Magnetostratigraphically, Els Nerets locality is correlated with the magnetochrone C31r and biostratigraphic and lithostratigraphic correlations indicate a lower Maastrichtian age for Els Nerets, ca. 70 Ma (Fondevilla et al., 2017; 2019).

## *2.2 Faunal content*

The Els Nerets locality was first discovered and excavated in 1984 (Casanovas et al., 1987; Buscalioni et al., 1986), a second research phase started in 2003 with a series of prospections and excavations (Gaete et al., 2003) and later with systematic excavations from

2013 to 2018. During these years dozens of specimens were collected, revealing a diverse fauna. The locality has yielded plant remains, teeth and scales of fishes, bones of turtles, bones and teeth of crocodiles, teeth of indeterminate theropod, teeth and bones of titanosaur sauropods, osteoderms of indeterminate ankylosaurians and bones and tracks of hadrosaurids. The earliest finding of hadrosaurid bones at this locality were formerly referred to the genus “Orthomerus” (Casanovas-Cladellas et al., 1985), currently a *nomen nudum* (Brinkmann, 1988; Horner et al., 2004).

The bones are found at the base of a one metre thick marly limestone bed of the lower Maastrichtian La Posa Formation. The skeletal elements recovered in the 2013–2018 fieldwork seasons were found disarticulated and their orientation was given by the angle between the north and the major axis of the bones. After plotting the bones in a 180° rose diagram in order to determine the main direction of flow that transported the fossil elements, 29 bones revealed a mean orientation of 70.65° to the azimuth, with a circular standard deviation of 54.21°, and a 95% confidence interval of 90.78° and 50.53° (Fig. 3). The relatively low circular variance (0.36, where 0 is unimodal and 1 evenly distributed around a circle) supports the predominant unidirectional deposition of the bones (Morris et al., 1996). The distal portions of some bones are eroded or broken (e.g. the distal portion of the femur MCD-4698, Fig. 7), while other elements preserve delicate structures (e.g. the obturator process of the ischium MCD-6689, Fig. 6B). The different preservation state of the bones suggests that the depositional event was driven by a quick unidirectional flow (Morris et al., 1996).

### 3. Material and methods

#### 3.1. Material



The hadrosaurid remains collected from Els Nerets consists of a partial dentary tooth (MCD-5214), six partial dorsal vertebrae (MCD-8632, MCD-8633, MCD-8634, MCD-8635, MCD-8636, MCD-8637), a sacral centrum (MCD-64), two fused sacral centra (MCD-7027), complete proximal caudal vertebra (MCD-8638), complete caudal vertebrae (MCD-6690, IPS-NE-13), seven partial caudal vertebrae (MCD-61, MCD-62, MCD-63, MCD-65, MCD-66, MCD-5209, MCD-7095), complete left humerus (MCD-6691), right ulna (MCD-8640), fragment of left radius (MCD-5208), fragment of left ilium (MCD-8639), nearly complete right ischium (MCD-6689), partial left ischium (MCD-7032), two complete right femora (MCD-4698, 7033), partial distal half of right femur (IPS-896), distal epiphysis of left femur (MCD-6743b), partial right fibula (MCD-6688), and fragmentary right metatarsal IV (MCD-5203). The material belongs to at least three individuals, based on the recovery of a maximum of three right femora.

### *3.2. Phylogenetic analysis*

The phylogenetic position of the Els Nerets lambeosaurine was inferred using Maximum Parsimony analysis. The taxonomic sample included 16 non hadrosaurid-hadrosauroids, 23 Saurolophinae and 24 Lambeosaurinae. We used the character-taxon matrix of Prieto-Márquez et al. (2019), to which we added five new characters (Appendix), totalling 285 morphological characters (195 cranial and 90 postcranial; see supplementary data 1 and 2). The tree search was conducted in TNT version 1.5 (Goloboff and Catalano, 2016). A heuristic search of 10,000 replicates using random addition sequences was performed, followed by branch swapping by tree bisection reconnection holding ten trees per replicate. Multistate characters containing states that are not mutually exclusive, following a natural morphocline, were ordered. Bootstrap proportions (Felsenstein, 1985) were calculated using TNT, setting the analysis for 5,000 replicates using heuristic searches, in which each search

was conducted using random additional sequences with branch-swapping by subtree pruning and regrafting and 25 replicates.

## **4. Results**

### *4.1. Cranial elements*

The only cranial element recovered at Els Nerets, MCD-5214, is a dentary tooth crown missing the apical region (Fig. 4). The tooth crown is diamond-shaped, as is typical of hadrosaurids (Prieto-Márquez, 2010), slightly asymmetrical and gently curved caudally. Assuming that the dorsal half of the crown was as tall as the preserved ventral half, the element was about three times taller than wide at mid-height. The enamelled surface bears a single median ridge the lingual margin of which is eroded away along its dorsal extent. Two or three short fainter accessory ridges are present on each side of the much larger and robust median ridge (Fig. 4B). These fainter ridges are obliquely oriented relative to the median ridge and disappear before mid-height of the tooth crown. Marginal papillae are relatively small and subrectangular (Fig. 4A).

### *4.2. Axial elements*

#### *4.2.1. Dorsal Vertebrae*

Dorsal centra (MCD-8632–MCD-8637; Table 1) are slightly opisthocoelous, gently compressed craniocaudally and mediolaterally, and with heart-shaped cranial and caudal articular surfaces (Fig. 5A and B). The description is based on the vertebra MCD-8633. The neural arch is fused to the centra. The neural canals are elliptical, more expanded dorsoventrally than mediolaterally. The prezygapophyses are elliptical facets oriented

craniodorsally laying near the craniodorsal margin of the neural arch. The transverse processes are elliptical in cross section and show a well developed ventral ridge. The ridge is attached medially to the transverse process and expands caudoventrally, articulating with the caudal margin of the neural arch. Most postzygapophyses are incompletely preserved and are oriented caudoventrally. Between the postzygapophyses there is a sulcus on the caudal margin of the neural spine. The neural spine lacks the distal portion and it has a slight cranial offset. It has an elliptical section, with a height at least twice that of the centrum.

#### 4.2.2. *Sacrum*

The sacrum is incompletely known from a few fragmentary centra. MCD-7027 consists of two fused sacral centra (Fig. 5C–E). The dorsal surface preserves the peduncles of the neural arches. MCD-64 consists of a sacral centrum preserving portions of the neural arches and the attachment sites for the transverse processes (Fig. 5F–H). All these sacral centra are slightly wider than tall. They are slightly hourglass-shaped in ventral view, given that they are mediolaterally constricted at mid-length. The ventral surfaces of these centra are smooth and show no sulci.

#### 4.2.3. *Caudal Vertebrae*

MCD-8638 (Fig. 5I and J) is a proximal caudal vertebra exhibiting craniocaudally compressed and opisthocoelous centra, with concave lateral surfaces. The neural arch encloses an oval neural canal. Above and between both prezygapophyses, on the cranial surface of the base of the neural spine, there is a wide sulcus that narrows dorsally. The transverse processes are dorsoventrally expanded, craniocaudally compressed and slightly offset cranially. Dorsal to the neural canal, the postzygapophyses are elliptical facets and oriented ventrally. The neural spine is twice as tall as the centrum and it is caudally inclined along its proximal

segment 25° relative to the dorsoventral axis of the centrum. The neural spine is elliptical in cross section, thicker proximally than distally. On the cranial surface of the neural spine there is a sulcus above the prezygapophyses that extends to mid-height of the neural spine.

IPS-NE-13 (Fig. 5K and L) preserves the amphicoelous centrum of a mid-caudal vertebra. This centrum displays hexagonal cranial and caudal facets, and concave lateral and ventral surfaces. The ventral surface preserves the articular facets for the haemal arches. The lateral surfaces bear approximately square facets for attachment of the transverse processes. These facets are more expanded craniocaudally than dorsoventrally. The proximal segment of the neural arch is caudally inclined and encloses a rounded neural canal. The prezygapophyses are cranially projected with craniomedially oriented articular facets. Dorsomedial to the prezygapophyses, on the cranial surface of the neural spine, there is a sulcus that extends to mid-height of the neural spine. The postzygapophyses are relatively small, located on the neural spine, dorsal to the neural canal and facing lateroventrally. The neural spine is slightly inclined caudally, missing its distal end and is less than twice the height of the centrum.

MCD-6690 is a highly distorted mid-caudal vertebra (Fig. 5M–P), diagenetically compressed mediolaterally. The centrum is amphicoelous and the proportions and dimensions of the articular facets have not been distorted. The lateral surfaces are concave. The right surface shows the articular facet for the transverse process. The ventral surface of the centrum is concave, with a smooth median sulcus. The neural arch is poorly preserved and encloses a rounded neural canal. Dorsal to the neural canal, the prezygapophyses show an oval shape and face craniodorsally. The neural spine is more than three times taller than the centrum and it expands and thickens distally. Dorsal to the prezygapophyses, on the cranial surface of the neural spine, there is a small sulcus (Fig. 5N). On the cranial surface of the neural spine, 5 cm above the attachment of the neural arch, there is a rounded and short protuberance that extends cranially (Fig. 5O and P). This feature is anomalous in that it is not present in any of

the other available vertebrae for which the neural spine is preserved, nor is it known in any other ornithopod for that matter. Given its anomalous shape and location, we suggest that it may be pathological. However, because the bone surface of this feature is smooth, as that of the lateral surface of the neural spine, it is likely not the result of bone fracture and remodelling, but rather perhaps an abnormality that might have been present from birth.

### *4.3. Appendicular elements*

#### *4.3.1. Humerus*

MCD-6691 is a well preserved left humerus (Fig. 6A–C) missing only small portions of the cranial margin of the deltopectoral crest. This is a particularly slender element, more than five times longer than wide (the width here being measured along the proximal margin of the lateral surface). This ratio makes MCD-6691 one of the more gracile humeri of a lambeosaurine. The lateral surface of the expanded proximal end describes a slightly concave outline in proximal view, with the proximal extent of the deltopectoral crest oriented craniolaterally. The deltopectoral crest accounts for 57% of the length of the humerus. The lateroventral expansion of the crest is 1.7 times the minimum diameter of the shaft. The shaft of the humerus exhibits a slightly sigmoidal profile in mediolateral view. Distally, the shaft expands both craniomedially and caudolaterally to form the distal condyles. The two condyles are oval in cross section, the radial condyle being slightly more robust than the ulnar condyle. The condyles are separated by a deep sulcus that is further developed caudally.

#### *4.3.2. Ulna*

MCD-8640 is an almost complete right ulna (Fig. 6D and E). It has a slender diaphysis, being more than 14 times longer than it is dorsoventrally thick. At the proximal end, the lateral and medial flanges are heavily eroded. The olecranon process is relatively thick mediolaterally and its proximal surface is abraded. The dorsal surface of the proximal segment of the ulna displays a shallow depression that occupies half the length of the bone. The diaphysis exhibits longitudinal shallow striated ligament scars. The distal end is eroded and shows an oval section.

#### 4.3.3. *Radius*

This element is solely represented by an eroded fragment of a left distal end (MCD-5208; Fig. 6F and G). The distal surface is subcircular. The distal-most region of the diaphysis is suboval in cross section and shows longitudinal striated ligament scars.

#### 4.3.4. *Ilium*

MCD-8639 is a proximal segment of the preacetabular process of a left ilium (Fig. 7A). The process is an elongate lamina that gradually becomes slightly shallower distally. The proximal extent of the preserved segment curves ventrally and is broken before reaching the craniodorsal margin of the pubic process of the ilium. On the medial surface there is a longitudinal ridge, a condition shared among all hadrosaurids (Prieto-Márquez 2010).

#### 4.3.5. *Ischium*

The right ischium MCD-6689 (Fig. 7B–E) is nearly complete, missing only the distal end. The element exhibits a ‘thumb-like’ iliac processes. The dorsal and ventral margins of the iliac process are convergent. The pubic process of MCD-6689 is relatively elongated, being as long as it is wide along its articular face. The obturator process appears relatively

long and thin due to erosion and breakage. The shaft of the ischium is relatively slender: its dorsoventral thickness at mid-length is 5.4% of its total length. A depression is present on the lateral surface of the proximal extent of the shaft. Ventrally, this depression is bounded by a sharp ridge. On the medial surface, there are several longitudinal ridges for the articulation with its counterpart.

The left ischium MCD-7032 is slightly distorted post-depositionally and lacks portions of the pubic and iliac processes, the obturator process and the distal end. The iliac process is ‘thumb-shaped’ in lateral profile and displays the same proportions as MCD-6689. On the lateral surface of the ischium, also as in MCD-6689, there is a depression. This depression is located caudal and ventral to the iliac process, delimited by a ridge at the level of the obturator process. The ischiatic shaft is slightly deformed, and on the medial surface there are ridges indicating articulation with its counterpart.

#### 4.3.6. Femur

The femur is the best represented appendicular element of the lambeosaurine from Els Nerets. The following description is mostly based on the two complete femora, MCD-7033 (Fig. 8A–B) and MCD-4698 (Fig. 8C–D). MCD-7033, previously referred to the nomen dubium *Orthomerus* (Casanovas et al., 1985), is a complete right femur, albeit diagenetically compressed mediolaterally. The articular head is compressed craniocaudally but preserves the dimension proximodistally. The fourth trochanter displays a symmetrical profile in lateral view and is continuous with the lateral margin of the shaft. The distal condyles, the more robust of which is the medial one, form an ‘H’ shape in distal view. The lateral condyle presents a concave lateral surface. The gentle curvature of the shaft and the symmetrical profile of the fourth trochanter demonstrate that referring this femur to the genus *Orthomerus* is erroneous,

since the femora of *Orthomerus dolloi* Selley, 1883, the only recognized species of the genus, show different features.

MCD-4698 is the best preserved femur from Els Nerets. It is comparable in size (length: 63 cm) with the medium sized femora from the Basturs Poble site (Dalla Vecchia et al., 2014; Fondevilla et al., 2018). The greater trochanter is craniocaudally expanded, with a concave lateral surface. The shaft has a gentle curvature and a squared cross section. The fourth trochanter is well preserved, with a symmetrical profile, and its length corresponds to 30% of the total length of the femur.

#### 4.3.7. Fibula

MCD-6688 is a rod-like right fibula (Fig. 8E–F), with a smooth curvature along the distal half of the bone. The proximal half of the shaft is slightly expanded, maintaining a triangular section that becomes circular distally.

#### 4.3.8. Metatarsal IV

MCD-5203 is a proximal fragment of a right metatarsal IV (Fig. 8G–H). Except for its dorsolateral surface, all other sides are eroded to the point of exposing the inner osseous texture. The partially preserved medial surface appears to have been gently depressed, for articulation with the metatarsal III. The incomplete distal portion displays a D-shaped section.

### 4.4. Phylogenetic relationships of the Els Nerets lambeosaurine

The Maximum Parsimony analysis resulted in 12 most parsimonious trees hitting a best score of 1071 steps for 1909 times out of 10000 replicates; with Consistency Index of 0.45 and Retention Index of 0.77. The consensus tree placed the Els Nerets lambeosaurine within Lambeosaurinae, forming a polytomic relationship with the basal lambeosaurine



species *Aralosaurus tubiferus*, *Canardia garonnensis*, *Jaxartosaurus aralensis*, *Tsintaosaurus spinorhinus*, *Pararhabdodon isonensis* and *Adynomosaurus arcanus* (Fig. 9).

Lambeosaurine synapomorphies present in the Els Nerets specimens consist of a long deltopectoral crest that is over 55% of the length of the humerus, and a recurved ‘thumb-like’ iliac process. The Els Nerets lambeosaurine shares with Tsintaosaurini a pubic process as long as its articular surface is wide, and an ischium with mid-shaft depth being less than 7.5% of the length of the shaft.

## 5. Discussion

### 5.1. Comparison with other lambeosaurines

The dorsal vertebrae of the Els Nerets lambeosaurine show a sulcus between the postzygapophyses on the caudal margin of the neural spine of the dorsal vertebrae, which is present in all members of the clade except *Amurosaurus riabini* Bolotsky & Kurzanov, 1991 (Godefroit et al., 2004). The height of the neural spine relative to the centrum of dorsal vertebrae is similar to those of most Lambeosaurinae, except *Magnapaulia laticaudus*, Prieto-Márquez et al., 2012 (e.g. LACM 17715), *Hypacrosaurus* spp. (e.g. MOR 549, CMN 8501) and *Arenysaurus ardevoli* Pereda-Suberbiola et al., 2009 (MPZ2008/268, Cruzado-Caballero et al., 2013), which display taller neural spines. The absence of a ridge on the cranial surface of the neural spine is shared with other lambeosaurines, such as *Tsintaosaurus spinorhinus* Young, 1958 (e.g. IVPP V725), *Parasaurolophus walkeri* Parks, 1922 (e.g. ROM 768), *Lambeosaurus lambei* Parks, 1923 (e.g. ROM 758) and *Hypacrosaurus* spp. (e.g. MOR 549, CMN 8501). Caudal vertebrae show relative proportions of the centrum and the neural spine that are similar to those described in other Lambeosaurinae, such as tsintaosaurins *Tsintaosaurus spinorhinus* (e.g. IVPP V725) and *Pararhabdodon isonensis* (IPS SRA 24,

Prieto-Márquez et al., 2006), and lambeosaurins *Corythosaurus* spp. (e.g. LACM 126137), *Lambeosaurus lambei* (e.g. ROM 758) and *Parasaurolophus* spp. (e.g. ROM 768, FMNH P27393). On the cranial surface of the neural spine, a sulcus above the prezygapophyses that extends to mid-height of the neural spine is shared with all other lambeosaurines, except *Olorotitan ararhensis* Godefroit et al., 2003 (e.g. AEMH 2/845, Godefroit et al., 2012).

In the humerus, a deltopectoral crest accounting for over 55% of its length is also present in most lambeosaurines (Prieto-Márquez 2010), with the exception of *Canardia garonnensis* (MDE-Ma3-20, Prieto-Márquez et al., 2013) and *Charonosaurus jiayinensis* (Godefroit et al., 2000). Similar proportions of the lateroventral expansion of the deltopectoral crest relative to the shaft diameter have been reported only in *Magnapaulia laticaudus* (e.g. LACM 17715, Prieto-Márquez et al., 2012) among lambeosaurines.

The ischia recovered from Els Nerets show a ‘thumb-like’ iliac process, a common character among Lambeosaurinae (Brett-Surman and Wagner, 2007). The length/width ratio is similar to that of all other lambeosaurines, with values between 1.5 and 2, except in *Parasaurolophus cyrtocristatus* Ostrom, 1961 (e.g. FMNH P27393) which is less than 1.5, and *Amurosaurus riabinini* (Godefroit et al., 2004) which is greater than 2. The dorsal and ventral margins of the iliac process are convergent, and the articular facet has a length/width ratio less than 0.7; these characters are different from *Adynomosaurus arcanus* (e.g. MCD-7139). The elongated pubic process is a condition only shared with *Tsintaosaurus spinorhinus* (e.g. IVPP V725) and *Parasaurolophus cyrtocristatus* (e.g. FMNH P27393). The proportions of shaft width at mid-length relative to its total length, having a ratio between 0.05 and 0.075, is a condition shared with *T. spinorhinus* (e.g. IVPP V725), *Hypacrosaurus stebingeri* Horner and Currie, 1994 (e.g. MOR 549), *Lambeosaurus lambei* (e.g. ROM 1218), *Olorotitan ararhensis* (e.g. AEMH 2/845), *Parasaurolophus walkeri* Parks, 1922 (e.g. ROM 768), *Sahalyania elunchunorum* Godefroit et al., 2008 (e.g. GMH W400-2) and *Velafrons*

*coahuilensis* Gates et al., 2007 (e.g. CPC-59). The depression on the lateral surface of the ischium is present in all lambeosaurines except *Magnapaulia laticaudus* (e.g. LACM 17715), *Velafrons coahuilensis* (uncatalogued ischium from Cerro del Pueblo Formation examined at the Museo del Desierto, Saltillo) and *Sahaliyana elunchunorum* (e.g. GMH W400-2).

## 5.2. Comparison with lambeosaurines from Europe

Unlike other European lambeosaurine species (e.g. Casanovas-Cladellas et al., 1993), the Els Nerets form is characterized by lacking a cranial ridge on the neural spine of dorsal vertebrae. Likewise, the overall length/width proportions of the humerus are different: a ratio greater than 5 is recovered in the Els Nerets lambeosaurine while it is smaller than 4.9 in *P. isonensis*. The Els Nerets lambeosaurine is characterized by having a length/width ratio of the articular facet of the ischiadic iliac process smaller than 0.7 and convergent margins of the iliac process, while *Adynomosaurus arcanus* is characterized by having a wider articular facet and divergent margins. The Els Nerets specimen shares three characters with the lambeosaurine from the nearby Moror locality (Brinkmann, 1984) and *Tsintaosaurus spinorhinus*, namely a length/width ratio of the iliac process between 1.5 and 2, convergent caudodorsal and acetabular margins of the iliac process, and a depression of the lateral surface of the proximal ischiadic shaft.

Dorsal and sacral vertebrae (for which the neural spine is preserved) from Els Nerets differ from those of *Arenysaurus ardevoli* in having neural spines that are 3.25 times taller than their centra, the absence of a ridge on the cranial surface of the neural spine of dorsal vertebrae, and a sulcus on the cranial surface of the neural spine of caudal vertebrae.

Prieto-Márquez and Wagner (2009) and Prieto-Márquez et al. (2013) diagnosed the tribe Tsintaosaurini based on maxillary characters, none of which are preserved in Els Nerets. However, the aforementioned ischiadic characters shared between Els Nerets and

*Tsintaosaurus* hint at a possible relationship between those two forms, although this is not unambiguously supported by phylogenetic analysis.

### 5.3 The arrival of lambeosaurines in Europe

The only European region where lambeosaurine dinosaurs have been reported is the Ibero-Armorican island (Pereda-Suberbiola et al., 2009; Cruzado-Caballero et al., 2010; Prieto-Márquez et al., 2013; Csiki et al., 2015; Fondevilla et al., 2019). Prieto-Márquez and Wagner (2009) and Prieto-Márquez et al. (2013) reported the presence in the late Maastrichtian of members of tsintaosaurin (*Pararhabdodon isonensis*) and aralosaurin (*Canardia garonnensis*) tribes, respectively. The authors inferred that they were Asian immigrants which apparently would have reached the Ibero-Armorican island via dispersal events at the end of the early Maastrichtian or during the late Maastrichtian (Prieto-Márquez et al., 2013). The occurrence of other lambeosaurines with their closest relatives in North America (Csiki et al., 2015) led some authors to speculate that several migratory events occurred in the late Maastrichtian: two bringing tsintaosaurins and aralosaurins from Asia (Prieto-Márquez et al. 2013) and two other events bringing parasaurolophins from Asia into Europe and North America (Cruzado-Caballero et al., 2013). Although tentative, the apparent affinity of the Els Nerets lambeosaurine with *Tsintaosaurus spinorhinus* may provide support for an early Maastrichtian arrival of tsintaosaurins in the region (about 4 My before the occurrence of the tsintaosaurine *Pararhabdodon* in the latest Maastrichtian) and therefore, the timing and palaeogeographic origin of the early migratory event.

Furthermore, the Els Nerets lambeosaurine represents the first occurrence of Lambeosaurinae in Europe, and in particular those with Asian affinities. The early Maastrichtian arrival of lambeosaurines in western Europe sets the timing of the ecological change and community reorganization occurring during the so-called “Maastrichtian dinosaur

turnover” (Vila et al. 2016). Subsequently, lambeosaurine hadrosaurids rapidly became the most abundant herbivorous group in the late early Maastrichtian (Vila et al., 2016). Interestingly, the appearance of lambeosaurine hadrosaurids in the late early Maastrichtian (around 70 Ma) coincides with marine isotopic events 4 and 5 of the Campanian-Maastrichtian Boundary Events (CMBE) that could have brought about an important sea level drop (up to 25 m) which in turn would have favoured the opening of passages between landmasses (Fondevilla et al., 2019).

## 6. Conclusions

We document and re-evaluate the affinities of the hadrosaurid material from the classic European locality of Els Nerets, in the Tremp Basin (Catalonia). This lambeosaurine represents the oldest record of this clade in Europe. Several pelvic characters indicate a possible relationship with the Asian *Tsintaosaurus*. This, combined with the updated chronostratigraphic position of the site (c. 70 Ma), provides support for the hypothesis that tsintaosaurins arrived in Europe no later than early Maastrichtian. Future studies should test the tsintaosaurin affinities of Els Nerets and other south Pyrenean hadrosaurids, and a long history of this lineage in western Europe.

## Acknowledgements

We thank Rodrigo Gaete, Fabio Marco Dalla Vecchia, Victor Fondevilla and Cristiano Dal Sasso for providing additional data on specimens collected from various localities at the eastern Tremp syncline and elsewhere in Europe. We are also grateful to the numerous volunteers who took part in the fieldwork at Els Nerets. Thanks also to two anonymous

reviewers whose comments improved the quality of the manuscript. This work was supported by the Ministry of Economy, Industry and Competitiveness of the Government of Spain, via the Ramón y Cajal Program [RyC-2015-17388] presented to A. P.-M. and a grant [CGL2016-73230-P] presented to A. G. Additional support was also provided by the CERCA Program of the Generalitat de Catalunya, and the University of Bristol through the Bob Savage Memorial Fund.

## Supplementary data

Supplementary data 1. Taxon-character state matrix used in the phylogenetic analysis.

## References

- Benton, M.J., Csiki, Z., Grigorescu, D., Redelstorff, R., Sander, P.M., Stein, K., Weishampel, D.B., 2010. Dinosaurs and the island rule: the dwarfed dinosaurs from Hateg Island. *Palaeogeography, Palaeoclimatology, Palaeoecology* 293, 438–454. doi: 10.1016/j.palaeo.2010.01.026
- Blanco, A., Szabó, M., Blasco-Lapaz, À., Marmi, J., 2017. Late Cretaceous (Maastrichtian) Chondrichthyes and Osteichthyes from northeastern Iberia. *Palaeogeography, Palaeoclimatology, Palaeoecology* 465, 278–294. doi: 10.1016/j.palaeo.2016.10.039
- Bolotsky, Y., Kurzanov, S.M., 1991. Gadosavry Priamuriy. *Geology of the Pacific Ocean Border*, 94–103.
- Brett-Surman, M.K., Wagner, J.R., 2007. Discussion of character analysis of the appendicular anatomy in Campanian and Maastrichtian North American hadrosaurids – variation and

516 ontogeny. In: Carpenter, K. (Ed.), *Horns and Beaks: Ceratopsian and Ornithopod*  
 517 *Dinosaurs*. Indiana University Press, Bloomington and Indianapolis, 135–169.  
 518 Brinkmann, W., 1984. Erster Nachweis eines Hadrosauriers (Ornithischia) aus dem unterem  
 519 Garumnium (Maastrichtium) des Beckens von Tremp (Provinz Lérida, Spanien).  
 520 *Paläontologische Zeitschrift* 58, 295–305.  
 521 Brinkmann, W., 1988. Zur Fundgeschichte und Systematik der Ornithopoden (Ornithischia,  
 522 Reptilia) aus der ober-Kreide von Europe. *Documenta Naturae* 45, 1–157.  
 523 Buffetaut, E., 2009. An additional hadrosaurid specimen (Dinosauria: Ornithischia) from the  
 524 marine Maastrichtian deposits of the Maastricht area. *Carnets de Géologie (L03)*, 1–4.  
 525 Canudo, J.I., Oms, O., Vila, B., Galobart, À., Fondevilla, V., Puértolas-Pascual, E., Sellés, A.  
 526 G., Cruzado-Caballero, P., Dinarès-Turell, J., Vicens, E., Castanera, D., Company, J.,  
 527 Burrell, L., Estrada, R., Marmi, J., and Blanco, A., 2016. The upper Maastrichtian  
 528 dinosaur fossil record from the southern Pyrenees and its contribution to the topic of the  
 529 Cretaceous-Palaeogene mass extinction event. *Cretaceous Research* 57, 540–551.  
 530 Casanovas-Cladellas, M.L., Santafé-Llopis, J.V., Sanz, J.L., Buscalioni, A., 1985.  
 531 *Orthomerus* (Hadrosaurinae, Ornithopoda) del Cretácico Superior del yacimiento de “Els  
 532 Nerets” (Tremp, España). *Paleontologia i Evolució* 19, 155–162.  
 533 Casanovas, M.L., Santafé-Llopis, J.V., Sanz, J.L., Buscalioni, A.D., 1987. Arcosaurios  
 534 (Crocodilia, Dinosauria) del Cretacico Superior de la Conca de Tremp (Lleida, España).  
 535 *Estudios Geologicos*, vol. extr. Galve-Tremp, 95–110.  
 536 Casanovas-Cladellas, M.L., Santafé-Llopis, J.V., Isidro-Llorens, A., 1993. *Pararhabdodon*  
 537 *isonense* n. gen. n. sp. (Dinosauria). Estudio morfológico, radiotomográfico y  
 538 consideraciones biomecanicas. *Paleontologia i Evolució* 26–27, 121–131.

539 Company, J., Cruzado-Caballero, P., Canudo, J.I., 2015. Presence of diminutive hadrosaurids  
540 (Dinosauria: Ornithopoda) in the Maastrichtian of the south–central Pyrenees (Spain).  
541 Journal of Iberian Geology 41, 71–81.

542 Cruzado-Caballero, P., Pereda-Superbiola, X., Ruiz-Omeñaca J.I., 2010. *Blasisaurus canudo*  
543 gen. et sp. nov., a new lambeosaurine dinosaur (Hadrosauridae) from the latest  
544 Cretaceous of Arén (Huesca, Spain). Canadian Journal of Earth Sciences 47, 1507–1517.

545 Cruzado-Caballero, P., Canudo, J.I., Moreno-Azanza, M., Ruiz-Omeñaca J.I., 2013. New  
546 material and phylogenetic position of *Arenysaurus ardevoli*, a lambeosaurine dinosaur  
547 from the Late Maastrichtian of Arén (Northern Spain). Journal of Vertebrate  
548 Paleontology 33, 1367–1384.

549 Csiki-Sava, Z., Buffetaut, E., Ósi, A., Pereda-Superbiola, X., Brusatte, S. L., 2015. Island life  
550 in the Cretaceous – faunal composition, biogeography, evolution, and extinction of land-  
551 living vertebrates on the Late Cretaceous European archipelago. ZooKeys, 469, 1–161.  
552 doi: 10.3897/zookeys.469.8439

553 Cuevas, J.L., 1992. Estratigrafía del “Garumniense” de la Conca de Tremp. Prepirineo de  
554 Lerida. Acta Geológica Hispánica 27, 95–108.

555 Dalla Vecchia, F.M., 2014. An overview of the latest Cretaceous hadrosauroid record in  
556 Europe. In: Eberth, D.A., Evans, D.C. (Eds.), Hadrosaurs. Indiana University Press,  
557 Indianapolis, 268–297.

558 Dalla Vecchia, F.M., Gaete, R., Riera, V., Oms, O., Prieto-Márquez, A., Vila, B., Sellés,  
559 A.G., Galobart, A., 2014. The hadrosauroid record in the Maastrichtian of the eastern  
560 Tremp Syncline (northern Spain). In: Eberth, D.A., Evans, D.C. (Eds.), Hadrosaurs.  
561 Indiana University Press, Indianapolis, 298–314.

562 Díez-Canseco, D., Arz, J.A., Benito, M., Diaz-Molina, M., Arenillas, I., 2014. Tidal influence  
563 in redbeds: a palaeoenvironmental and biochronostratigraphic reconstruction of the



564 Lower Tremp Formation (South-Central Pyrenees, Spain) around the Cretaceous/  
 565 Paleogene boundary. *Sedimentary Geology* 312, 31–49. doi:  
 566 10.1016/j.sedgeo.2014.06.008

567 Felsenstein, J., 1985. Confidence limits on phylogenies: an approach using the bootstrap.  
 568 *Evolution* 39, 783–791.

569 Fondevilla, V., Vincente, A., Battista, F., Sellés, A.G., Dinarès-Turell, J., Martínclonas, C.,  
 570 Anadón, P., Vila, B., Razzolini, N.L., Galobart, À., Oms, O., 2017. Geology and  
 571 taphonomy of the L’Espinau dinosaur bonebed, a singular lagoonal site from the  
 572 Maastrichtian of the South–Central Pyrenees. *Sedimentary Geology* 355, 75–92.

573 Fondevilla, V., Dalla Vecchia, F.M., Gaete, R., Galobart, À., Moncunill–Solé, B., Köhler, M.,  
 574 2018. Ontogeny and taxonomy of the hadrosaur (Dinosauria, Ornithopoda) remains from  
 575 Basturs Poble bonebed (late early Maastrichtian, Tremp syncline, Spain). *PLoS ONE*  
 576 13(10): e0206287. doi: 10.1371/journal.pone.0206287

577 Fondevilla, V., Riera, V., Vila, B., Sellés, A.G., Dinarès-Turell, J., Vicens, E., Gaete, R.,  
 578 Oms, O., Galobart, À., 2019. Chronostratigraphic synthesis of the latest Cretaceous  
 579 dinosaur turnover in south–western Europe. *Earth-Science Reviews* 191, 168–189. doi:  
 580 10.1016/j.earscirev.2019.01.007

581 Gates, T.A., Sampson, S.D., Delgado de Jesus, C.R., Zanno, L.E., Eberth, D., Hernandez-  
 582 Rivera, R., Aguillon-Martinez, M.C., 2007. *Velafrons coahuilensis*, a new  
 583 lambeosaurine hadrosaurid (Dinosauria: Ornithopoda) from the Late Campanian Cerro  
 584 del Pueblo Formation, Coahuila, Mexico. *Journal of Vertebrate Paleontology* 27, 917–  
 585 930.

586 Godefroit, P., Zan, S., Jin, L., 2000. *Charonosaurus jiayinensis* n. g., n. sp., a lambeosaurine  
 587 dinosaur from the Late Maastrichtian of northeastern China. *Comptes Rendus de*  
 588 *l’Academie des Sciences, Paris, Sciences de la Terre et des Planètes* 330, 875–882.

589 Godefroit, P., Bolotsky, Y., Alifanov, V., 2003. A remarkable hollow-crested hadrosaur from  
590 Russia: an Asian origin for lambeosaurines. *Comptes Rendus Palevol* 2, 143–151.

591 Godefroit, P., Bolotsky, Y.L., van Itterbeek, J., 2004. The lambeosaurine dinosaur  
592 *Amurosaurus riabini*, from the Maastrichtian of Far Eastern Russia, *Acta Palaeontologica*  
593 *Polonica* 49, 585–618.

594 Godefroit, P., Sjulín, H., Tingxiang, Y., Lauters, P., 2008. New hadrosaurid dinosaurs from  
595 the uppermost Cretaceous of northeastern China. *Acta Palaeontologica Polonica* 53, 47–  
596 74.

597 Godefroit, P., Bolotsky, Y.L., Bolotsky, I.Y., 2012. Osteology and relationships of *Olorotitan*  
598 *arharensis*, a hollow-crested hadrosaurid dinosaur from the latest Cretaceous of Far  
599 Eastern Russia. *Acta Palaeontologica Polonica* 57, 527–560.

600 Goloboff, P.A., Farris, J.S., Nixon, K.C., 2008. TNT, a free program for phylogenetic  
601 analysis. *Cladistics* 24, 774–786.

602 Horner, J.R., Currie, P.J., 1994. Embryonic and neonatal morphology and ontogeny of a new  
603 species of *Hypacrosaurus* (Ornithischia, Lambeosauridae) from Montana and Alberta.  
604 *Dinosaur Eggs and Babies*, Cambridge University Press, Cambridge, 312–336.

605 Horner, J.R., Weishampel, D.B., Forster, C.A., 2004. Hadrosauridae. In: Weishampel, D.B.,  
606 Dodson, P., Osmólska, H. (Eds.), *The Dinosauria*, Second Edition. University of  
607 California, Berkeley, 438–463.

608 Kovach, W., 2018. Oriana version 4.02. Kovach Computing Services, Anglesey, Wales.

609 Mey, P.H., Nagtegaal, P.J.C., Roberti, K.J.A., Hartelvelt, J.J.A., 1968. Lithostratigraphic  
610 subdivision of posthercynian deposits in the south-central Pyrenees, Spain. *Leidse*  
611 *Geologische Mededelingen* 41, 221–228.

612 Morris, T.H., Richmond, D.R., Grimshaw, S.D., 1996. Orientation of dinosaur bones in  
 613 riverine environments: insights into sedimentary dynamics and taphonomy. In Morales,  
 614 M., ed., The Continental Jurassic: Museum of Northern Arizona Bulletin 60, 521–530.  
 615 Ostrom, J.H., 1961. A New Species of hadrosaurian dinosaur from the Cretaceous of New  
 616 Mexico. *Journal of Vertebrate Paleontology* 35, 575–577.  
 617 Parks, W.A., 1922. *Parasaurolophus walkeri*, a new genus and species of crested trachodont  
 618 dinosaur. University of Toronto Studies, Geology Series 13, 1–32.  
 619 Parks, W.A., 1923. *Corythosaurus intermedius*, a new species of trachodont dinosaur.  
 620 University of Toronto Studies, Geological Series 15, 1–57.  
 621 Pereda-Superbiola, X., Canudo, J.I., Cruzado-Caballero, P., Barco, J.L., López-Martínez, N.,  
 622 Oms, O., Ruiz-Omeñaca, J.L., 2009. The last hadrosaurid dinosaurs of Europe: a new  
 623 lambeosaurine from the uppermost Cretaceous of Aren (Huesca, Spain). *Comptes Rendus*  
 624 *Palevol* 8, 559–572.  
 625 Prieto-Márquez, A., 2010. Global phylogeny of Hadrosauridae (Dinosauria: Ornithischia)  
 626 using parsimony and Bayesian methods. *Zoological Journal of the Linnean Society* 15,  
 627 435–502.  
 628 Prieto-Márquez, A., Gaete, R., Rivas, G., Galobart, À., Boada, M., 2006. Hadrosaurid  
 629 dinosaurs from the Late Cretaceous of Spain: *Pararhabdodon isonensis* revisited and  
 630 *Koutalisaurus kohlerorum*, gen. et sp. nov. *Journal of Vertebrate Paleontology* 26, 929–  
 631 943.  
 632 Prieto-Márquez, A., Chiappe, L.M., Joshi, S.H., 2012. The lambeosaurine dinosaur  
 633 *Magnapaulia laticaudus* from the Late Cretaceous of Baja California, Northwestern  
 634 Mexico. *PLoS ONE* 7(6): e38207. doi: 10.1371/journal.pone.0038207  
 635 Prieto-Márquez, A., Dalla Vecchia, F.M., Gaete, R., Galobart, A., 2013. Diversity,  
 636 relationships, and biogeography of the lambeosaurine dinosaurs from the European

637 Archipelago, with description of the new aralosaurin *Canardia garonnensis*. PLoS ONE,  
 638 8(7), e69835. doi: 10.1371/journal.pone.0069835.  
 639 Prieto-Márquez, A., Fondevilla, V., Sellés, A.G., Wagner, J.R., Galobart, À., 2019.  
 640 *Adynomorsaurus arcanus*, a new lambeosaurine dinosaur from the Late Cretaceous Ibero-  
 641 Armorican Island of the European Archipelago, Cretaceous Research 95, 19–37.  
 642 Puértolas-Pascual, E., Arenillas, I., Arz, J.A., Calvin, P., Esquerro, L., García-Vicente, C.,  
 643 Pérez-Pueyo, M., Sánchez-Moreno, E.M., Villalaín, J.J., and Canudo, J.I., 2018.  
 644 Chronostratigraphy and new vertebrate sites from the upper Maastrichtian of Huesca  
 645 (Spain), and their relation with the K/Pg boundary. Cretaceous Research 89, 36–59.  
 646 Riera, V., Oms, O., Gaete, R., Galobart, À., 2009. The end-Cretaceous dinosaur succession in  
 647 Europe: the Tremp Basin record (Spain). Palaeogeography, Palaeoclimatology,  
 648 Palaeoecology 283, 160–171. doi: 10.1016/j.palaeo.2009.09.018  
 649 Rosell, J., Linares, R., Llompart, C., 2001. El “Garumniense” prepirenaico. Revista de la  
 650 Sociedad Geológica de España 14, 47–56.  
 651 Torices, A., Barroso-Barcenilla, F., Cambra-Moo, O., Pérez-García, A., Segura, M., 2012.  
 652 Palaeontological and palaeobiogeographical implications of the new Cenomanian site  
 653 “Algora”. Cretaceous Research 37, 231–239. doi: 10.1016/j.cretres.2012.04.004  
 654 Vila, B., Sellés, A.G., Brusatte, S.L., 2016. Diversity and faunal changes in the latest  
 655 Cretaceous dinosaur communities of southwestern Europe. Cretaceous Research 57, 552–  
 656 564. doi: 10.1016/j.cretres.2015.07.003  
 657 Villalba-Breva, S., Martín-Closas, C., 2013. Upper Cretaceous paleogeography of the Central  
 658 Southern Pyrenean Basins (Catalonia, Spain) from microfacies analysis and charophyte  
 659 biostratigraphy. Facies 59, 319–345.  
 660 Young, C.C., 1958. The dinosaurian remains of Laiyang, Shantung. Palaeontologia Sinica,  
 661 New Series C 42, 1–138.

662  
663  
664  
665  
666  
667  
668  
669  
670  
671  
672  
673  
674  
675  
676  
677  
678  
679  
680  
681

## **Appendix**

New characters added to the character-taxon matrix of Prieto-Márquez et al. (2019) used in the phylogenetic analysis.

281. Presence or absence of ridge on the cranial surface of the neural spine of the caudal half of the dorsal vertebrae: absent (0); present (1).

282. Presence or absence of sulcus on the caudal surface of the neural spine of the caudal half of the dorsal vertebrae: absent (0); present (1).

283. Presence or absence of sulcus on the cranial surface on the neural spine of the cranial half of the caudal vertebrae: absent (0); present (1).

284. Presence or absence of depression on the lateral surface of the proximal region of the ischium. Lateral depression of the ischium: absent (0); present on the lateral surface of the ischiadic shaft (1); depression expanded in the proximal region of the ischium (2).

285. Offset of the lateral malleolus of the tibia, measured as the angle between the distal surface of the tibia and the long axis of the bone: angle greater than 12° (0); angle smaller than 12° (1).

## Figure captions

**Fig. 1.** Geographical and geological location of Els Nerets site. A, geographic location of the Tremp Basin (indicated by the shaded rectangle) in the Pyrenees. B, location of the main hadrosaurid-bearing sites in the Eastern Tremp Basin.

Intended for a 2-column fitting image.

**Fig. 2.** Simplified stratigraphic section of the Tremp area showing the position of Els Nerets site and other localities yielding lambeosaurine fossils.

Intended for a 2-column fitting image.

**Fig. 3.** Quarry map of Els Nerets site showing the spatial distribution of the recovered lambeosaurine skeletal remains. The insert diagram shows the statistical distribution of the angles of orientation of the fossil bones was analysed using the Orana 4.02 software (Kovach, 2018), with a mean orientation of  $70.65^{\circ}$  to the azimuth and the 95% confidence interval.

Intended for a 2-column fitting image.

**Fig. 4.** The only cranial element recovered from of Els Nerets lambeosaurine. A and B, dentary tooth (MCD-5214) in side and lingual views, respectively.

**Fig. 5.** Axial elements of the lambeosaurine from Els Nerets. A and B, dorsal vertebra (MCD-8633) in cranial and caudal views, respectively. C–E, pair of fused sacral centra (MCD-7027)

in dorsal, right lateral and ventral views, respectively. F–H, sacral centrum (MCD-64) in caudal, left lateral and ventral views, respectively. I and J, proximal caudal vertebra (MCD-8638) in cranial and left lateral views, respectively. K and L, mid-caudal vertebra (IPS-NE-13) in cranial and right lateral views, respectively. M, mid-caudal vertebra (MCD-6690) in left lateral view. N, dorsocraniolateral view of the prezygapophyseal region of MCD-6690, showing the sulcus on the cranial surface at the base of the neural spine, between the prezygapophyses. O and P, detail of the abnormal, possibly pathological growth of MCD-6690 in craniodorsal and left lateral views, respectively.

Intended for a 2-column fitting image.

**Fig. 6.** Forelimb elements of *Els Nerets lambeosaurine*. A–C, left humerus (MCD-6691) in medial, cranial, and caudolateral views, respectively. D and E, right ulna (MCD-8640) in lateral and dorsal views, respectively. F and G, distal fragment of left radius (MCD-5208) in dorsal and distal views, respectively.

Intended for a 2-column fitting image.

**Fig. 7.** Pelvic elements of *Els Nerets lambeosaurine*. A, preacetabular process of a left ilium (MCD-8639) in lateral view. B, right ischium (MCD-6689) in lateral view. C, line drawing of B. D, detail of MCD-6689 in caudoventrolateral view showing the lateral depression. E, line drawing of D.

Intended for a 2-column fitting image.

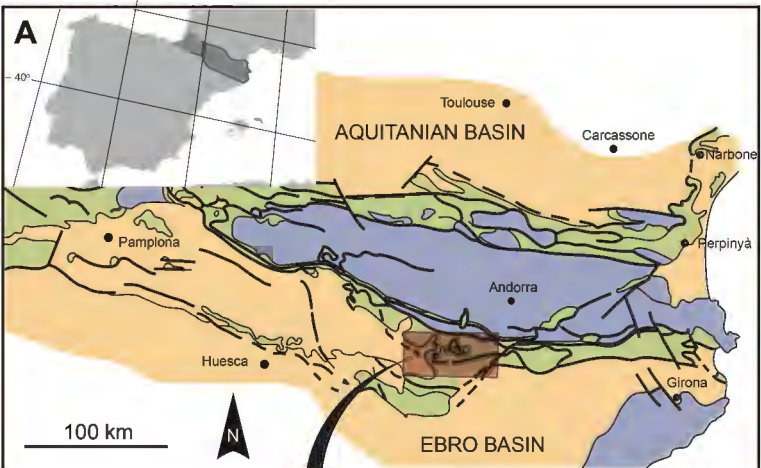
**Fig. 8.** Hindlimb elements of *Els Nerets lambeosaurine*. A and B, right femur (MCD-7033) in caudolateral and cranial views, respectively. C and D, right femur (MCD-4698) in caudal and craniomedial views, respectively. E and F, right fibula (MCD-6688) in caudal and cranial views, respectively. G and H, proximal fragment of right metatarsal IV (MCD-5203) in medial and proximal views, respectively.

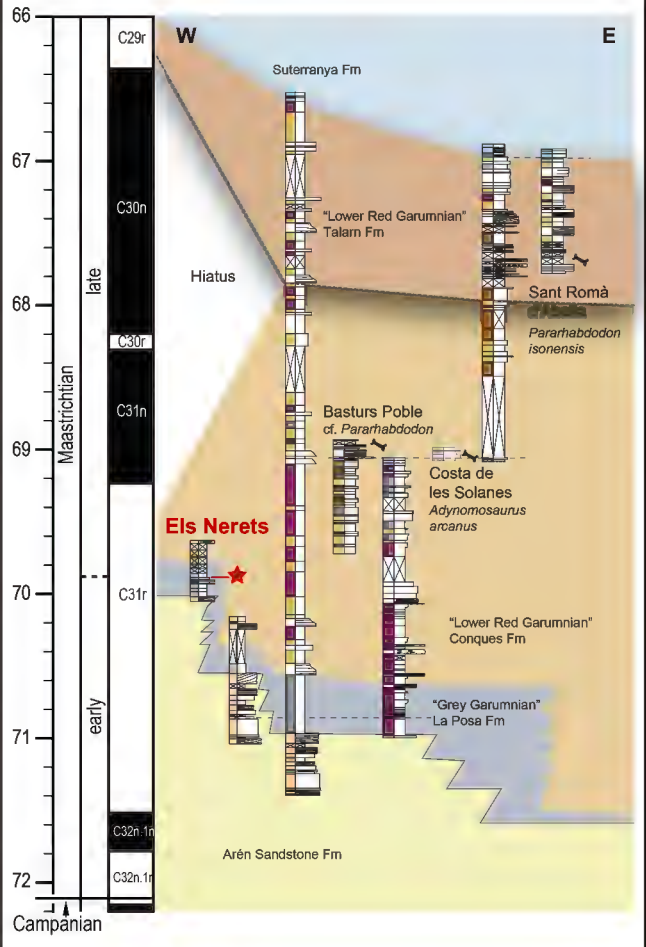
Intended for a 2-column fitting image.

**Fig. 9.** Phylogenetic relationships of *Els Nerets lambeosaurine*. Shown is the strict consensus tree of the 12 most parsimonious trees resulting from the parsimony analysis. Numbers below branches are Bootstrap proportions.

Intended for a 2-column fitting image.



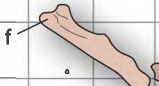
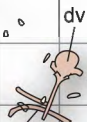
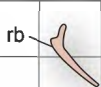
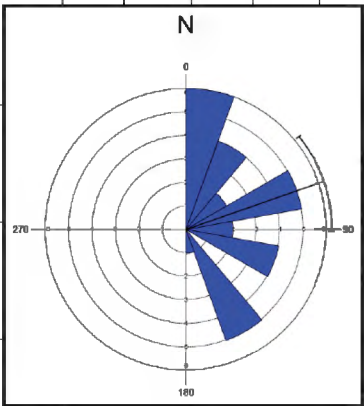






Lambeosaurinae

Other remains



50 cm

**A**

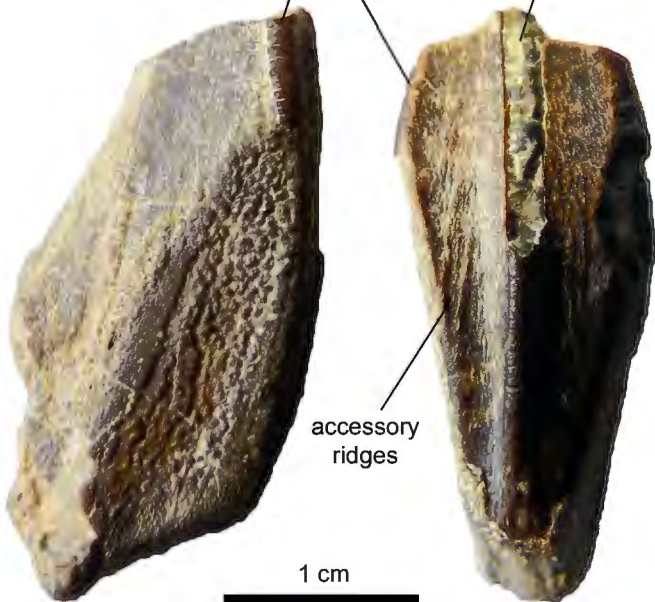
marginal papillae

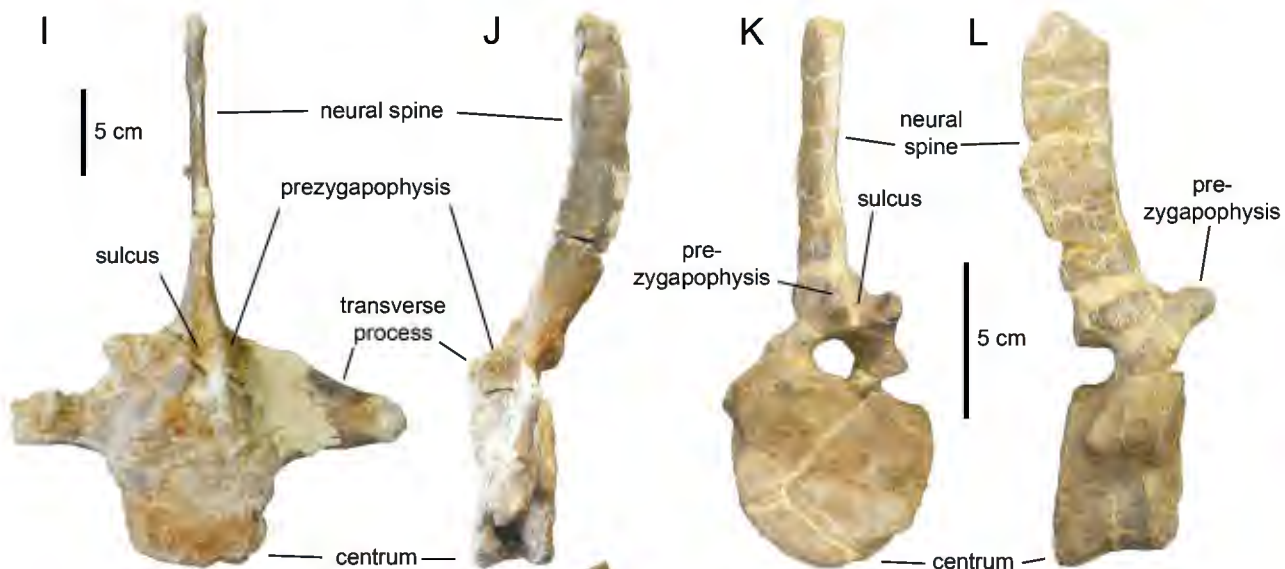
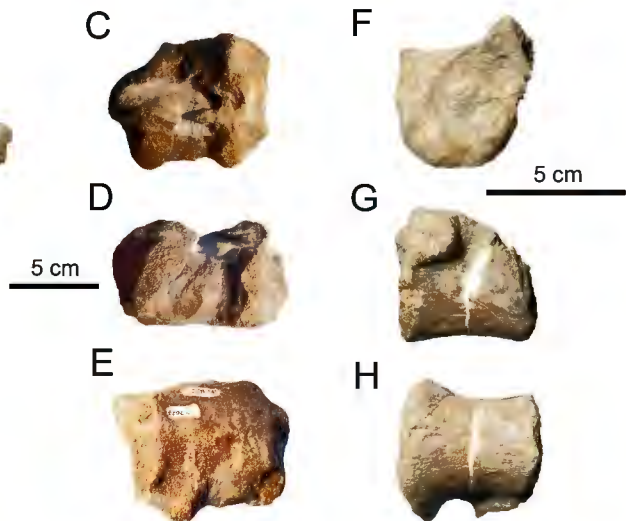
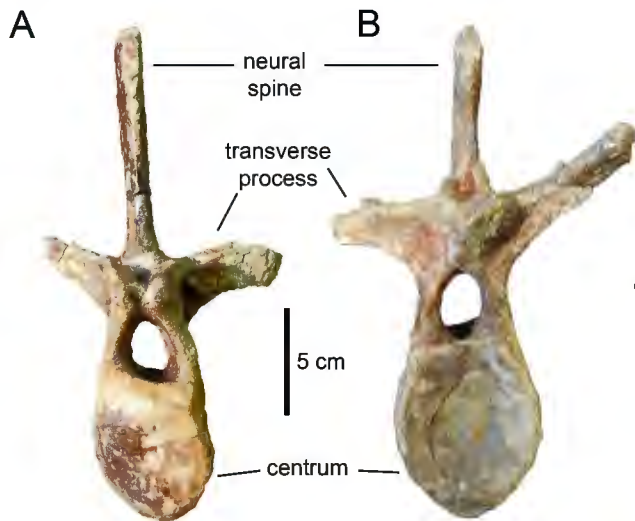
**B**

median  
ridge

accessory  
ridges

1 cm







**A**

articular head

**B**

articular head

deltopectoral crest

shaft

radial condyle

ulnar condyle

**C**

articular head

deltopectoral crest

10 cm

shaft

radial condyle

ulnar condyle

**D**

olecranon process

lateral flange



10 cm

**E**

medial flange

olecranon process

lateral flange

**F**

distal facet

**G**

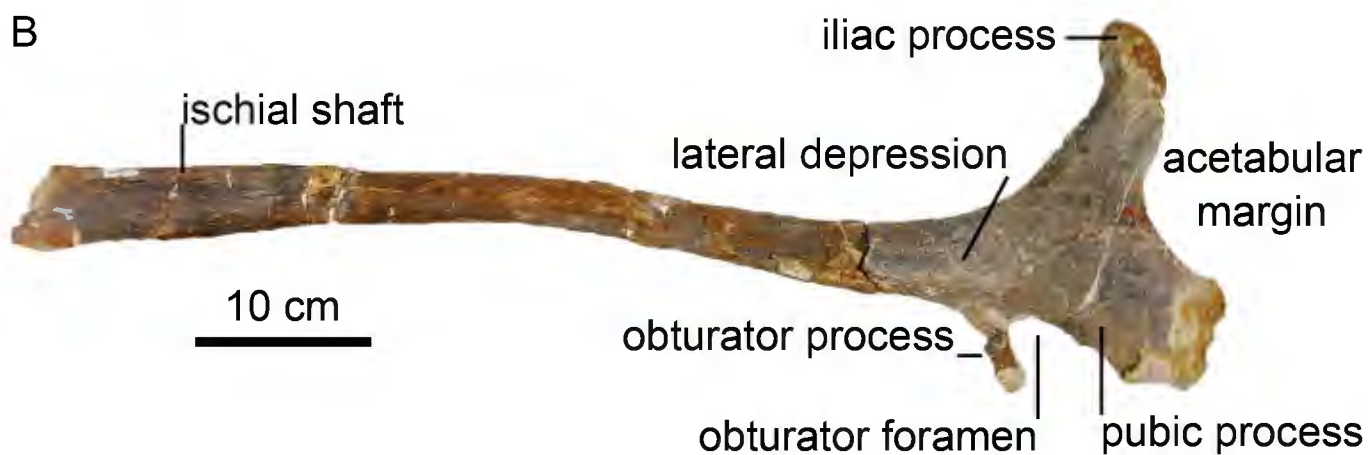
distal facet

5 cm

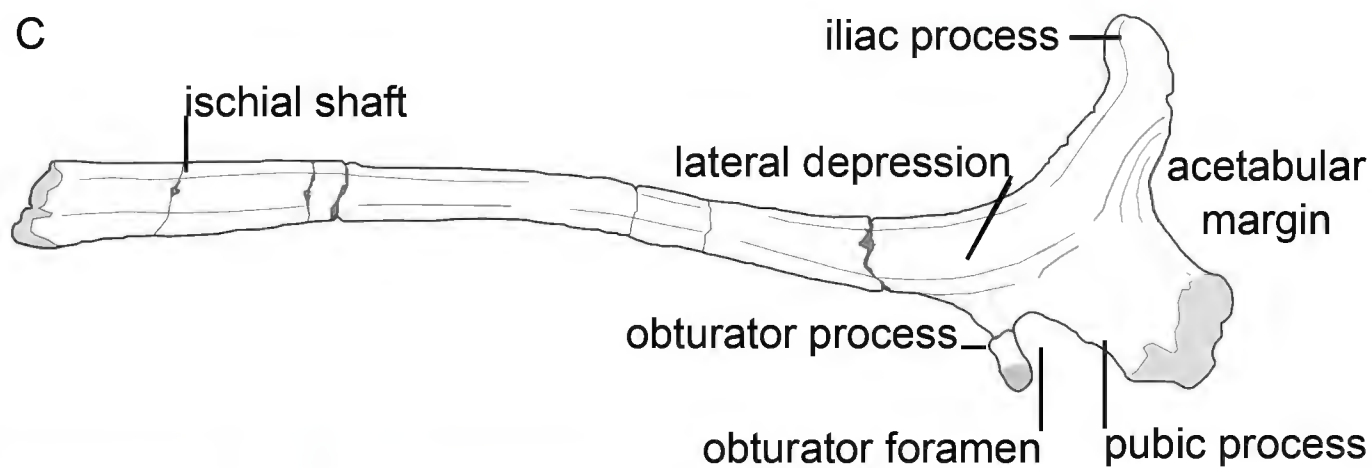
A



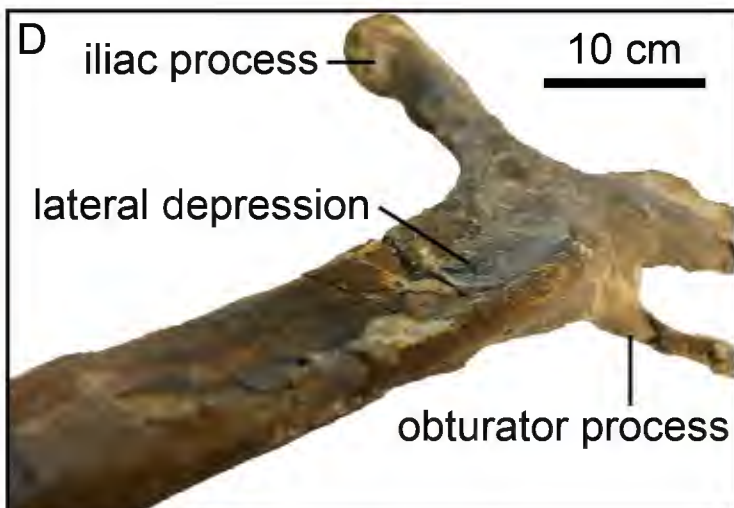
B



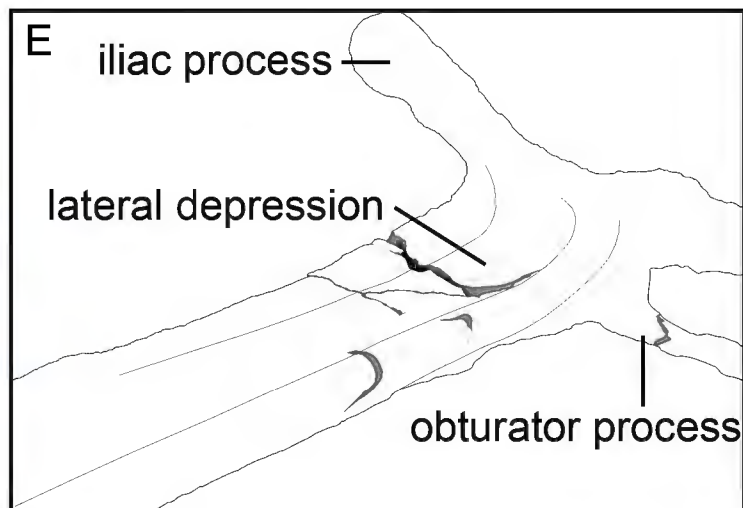
C

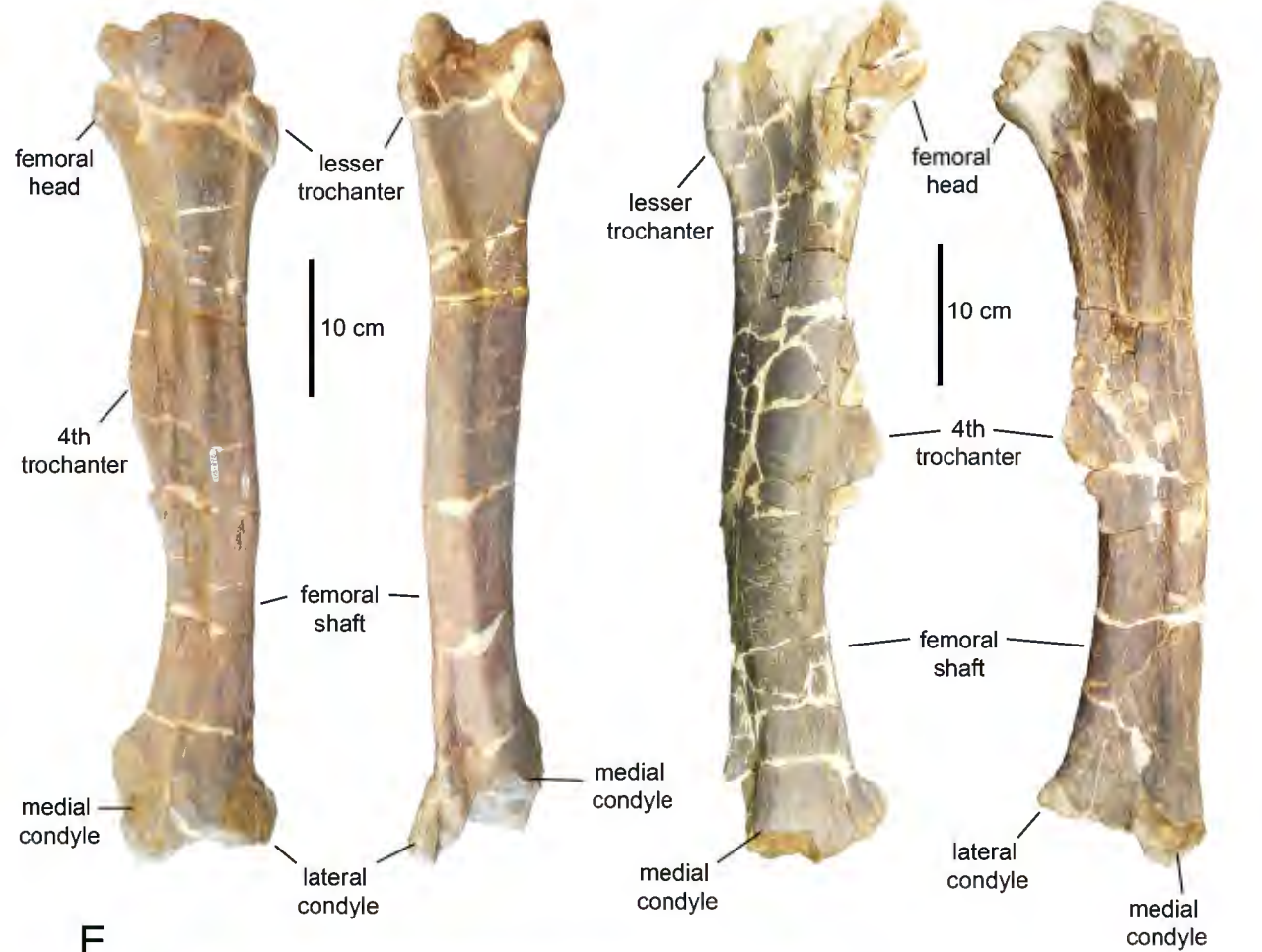


D



E



**A****B****C****D****E****F****G****H**